Journal of Pharmaceutical Analysis 9 (2019) 163–169

Contents lists available at ScienceDirect

Journal of Pharmaceutical Analysis

journal homepage: www.elsevier.com/locate/jpa

Original Article

# Development and validation of an LC-MS/MS method for tyrphostin A9

Lyndsey F. Meyer, Dhaval K. Shah*

*Department of Pharmaceutical Sciences, School of Pharmacy and Pharmaceutical Sciences, The State University of New York at Buffalo, Buffalo, NY 14214, USA*

ARTICLE INFO

*Article history:*
Received 29 October 2018
Received in revised form
7 March 2019
Accepted 7 March 2019
Available online 8 March 2019

*Keywords:*
Tyrphostin 9/ A9/AG-9/Malonoben/SF6847
LC-MS/MS
Stability
Pharmacokinetics
Tyrosine kinase inhibitor

ABSTRACT

Here we have presented a sensitive and selective LC-MS/MS method for the quantification of tyrphostin A9, which is a selective inhibitor for platelet derived growth factor receptor tyrosine kinase and has been investigated in vitro as a potent oxidative phosphorylation uncoupler. The murine analytical method was developed for three biological matrices: cell culture media, 3T3-L1 cell lysate, and murine plasma. For each matrix the limit of detection and the limit of quantification were found to be 0.5 ng/mL and 1.0 ng/mL, respectively. The range of standard curve for each matrix was 1.0–100 ng/mL, linearity was >0.99, and the precision and accuracy were within 20%. 3-(3,5-di-*tert*-butyl-4-hydroxyphenyl) propanoic acid was found to be the most suitable internal standard. The validated LC-MS/MS method was used to investigate stability and in vitro pharmacokinetics of tyrphostin A9. It was found that tyrphostin A9 is susceptible to hydrolysis, and the degradation product was identified as 3,5-di-*tert*-butyl-4-hydroxybenzaldehyde. Tyrphostin A9 was not stable in biological matrices, and the rate of its degradation in murine plasma was faster than that in cell culture media. In vitro pharmacokinetic studies revealed that tyrphostin A9 concentrations in the cell culture media declined in a bi-exponential manner and the concentrations inside the adipocytes remained constant, suggesting tyrphostin A9 has an intracellular binding site and is retained within the cell. The LC-MS/MS method presented here paves the way for further quantitative investigations involving tyrphostin A9.



## 1. Introduction

Tyrphostin A9 belongs to the class of synthetic tyrphostin compounds that are developed as a series of tyrosine kinase inhibitors with increased affinity for the epidermal growth factor receptor kinase domain [1]. A few selected tyrosine kinase inhibitors, such as AG1478 and AG 1417, have been investigated in preclinical models as anti-cancer agents [2–4]. While tyrphostin A9 has not yet been evaluated in a preclinical model, it has been investigated in vitro as an anti-oxidant, oxidative phosphorylation uncoupler, anti-viral, Pyk2 inhibitor, and selective inhibitor of platelet derived growth factor receptor tyrosine kinase [5–10]. However, despite many in vitro applications of tyrphostin A9, there is a lack of information regarding the stability and pharmacokinetics in various conditions.

Previous work performed by Won [11] evaluated the kinetics and mechanism of hydrolysis for a select series of tyrphostins. As described by Won, tyrphostins contain a characteristic carbon-carbon double bond activated by the cyano electron withdrawing group. Utilizing HPLC methodologies, Won characterized the methylene and aldehyde degradation products of hydrolysis for select tyrphostins [11]. Our interest in evaluating the stability of tyrphostin A9 stems from its oxidative phosphorylation uncoupling properties. Tyrphostin A9 is the most potent oxidative phosphorylation uncoupler known to date, with an effective concentration of 10 nM in isolated rat liver mitochondria, which is 5000 fold lower than the effective concentration of 2,4-dinitrophenol (an uncoupler and 1930s weight loss agent) [12]. We hypothesize that tyrphostin A9 has the potential to be a targeted anti-obesity agent by exploiting its uncoupling properties. To facilitate further therapeutic development of this molecule, we have developed and validated a liquid chromatography and tandem mass spectrometry (LC-MS/MS) method in three different biological matrices: cell culture media, 3T3-L1 cell lysate and murine plasma. This method was then used to investigate benchtop stability, in vitro

Peer review under responsibility of Xi'an Jiaotong University.
* Corresponding author.
*E-mail address:* dshah4@buffalo.edu (D.K. Shah).

https://doi.org/10.1016/j.jpha.2019.03.003

pharmacokinetics, and potential degradation products of tyrphostin A9.

## 2. Materials and methods

### 2.1. Reagents and chemicals

Tyrphostin A9, formic acid and 3,5-di-*tert*-butyl-4-hydroxybenzaldehyde were obtained from Sigma Aldrich (St. Louis, MO). 3-(3,5-di-*tert*-butyl-4-hydroxyphenyl) propanoic acid was acquired from Aurum Pharmatech (Franklin Park, NJ). Ultrapure water was purified using a Barnstead Nanopure Diamond system from Thermo Fisher Scientific (Watham, MA). Acetonitrile, dimethyl sulfoxide (DMSO) and acetic acid were purchased from Fisher Scientific (Watham, MA). 3T3-L1 cells were obtained from American Type Culture Collection and differentiated as previously described [13]. Phenol red free high glucose Dulbecco's modified eagle medium (DMEM), and insulin were purchased from Life Technologies (Grand Island, NY). Hyclone fetal bovine serum (FBS) was acquired from GE Life Sciences (Marlborough, Massachusetts).

### 2.2. Standard preparation

Standards and quality controls (QCs) were prepared in three matrices: high glucose DMEM phenol red free medium with insulin and 10% FBS, murine plasma containing EDTA, and 3T3-L1 cell lysate. Matrices were spiked with a stock solution of tyrphostin A9 prepared in DMSO and diluted in water to obtain final concentrations of 0.5, 1, 10, 50, and 100 ng/mL. QCs were prepared in a similar fashion for final concentrations of 3, 15, and 75 ng/mL. QCs were then extracted and stored at −20 °C to emulate storage conditions of samples.

### 2.3. Extraction procedures

#### 2.3.1. Cell culture medium

Phenol red free DMEM was spiked with 30 ng/mL of tyrphostin A9 and incubated in the presence of differentiated 3T3-L1 adipocytes (37 °C, 5% $CO_2$) in 6-well cell culture plates. 180 μL of medium was sampled from each well and transferred to 1.5 mL microcentrifuge tubes. 20 μL of 3-(3,5-di-*tert*-butyl-4-hydroxyphenyl) propanoic acid as an internal standard (IS) was added to each sample for a final concentration of 100 ng/mL prior to the extraction. Liquid-liquid extraction and protein precipitation were performed by adding 500 μL acetonitrile with 0.1% formic acid. Samples were then vortexed and centrifuged at 13,500 rcf at 4 °C for 10 min. 500 μL of supernatant was transferred to glass test tubes for drying under nitrogen. Samples were reconstituted in 200 μL acetonitrile +0.1% acetic acid and transferred to amber HPLC vials with 200 μL inserts for LC-MS/MS analysis.

#### 2.3.2. 3T3-L1 cell lysate

Differentiated 3T3-L1 adipocytes were cultured for up to 14 days in 6-well culture plates. At time 0, the medium was removed and fresh media containing tyrphostin A9 at a concentration of 30 ng/mL was added to the cells. Cells were incubated with medium containing tyrphostin A9 for 1, 3, 6 and 24 h. The cells were then washed twice with phosphate buffered saline (PBS) and incubated with 500 μL of 0.25% trypsin at 37 °C for 5–10 min to facilitate dissociation from the cell culture plate. 500 μL of medium was added to each well to deactivate trypsin and the detached cells were transferred to a microcentrifuge tube. Suspended cells were then centrifuged at 1000 rpm for 5 min to form a cell pellet. After removing the supernatant, 180 μL of acetonitrile was added to each sample to facilitate extraction of tyrphostin A9 followed by the addition of 20 μL IS. Samples were then sonicated using a sonicating probe with an amplitude of 25%, pulsing 5 s on and 3 s off for a total of 15 s. Liquid-liquid extraction and protein precipitation were performed following sonication by adding 500 μL acetonitrile with 0.1% formic acid. Samples were then vortexed and centrifuged at 15,000 rcf to pellet any remaining proteins and cellular debris. 500 μL of each sample was transferred to a glass test tube and dried under nitrogen. Samples were reconstituted in 200 μL acetonitrile with 0.1% acetic acid and centrifuged at low speed to prevent the transfer of any insoluble material to HPLC vials.

#### 2.3.3. Murine plasma

Murine plasma with EDTA was spiked with various concentrations of tyrphostin A9 to assess stability of tyrphostin A9 in the plasma matrix. Standards were generated by diluting 20 μL of murine plasma with analytical grade purified water spiked with concentrations of 0.5, 1, 10, 50 and 100 ng/mL of tyrphostin A9 and 20 μL IS for a total volume of 200 μL. Liquid-liquid extraction and protein precipitation were performed by adding 500 μL acetonitrile with 0.1% formic acid. Samples were then vortexed and centrifuged at 13,500 rcf to pellet precipitated proteins. 500 μL of each sample was transferred to a glass test tube and dried under nitrogen gas. Samples were reconstituted in 200 μL acetonitrile +0.1% acetic acid and analyzed with the LC-MS/MS.

### 2.4. Stability conditions

In order to determine benchtop stability, several replicate samples were prepared in both cell culture medium and murine plasma. The stability samples were then exposed to several benchtop conditions, including exposure to light at room temperature, protection from light at room temperature, and 3 freeze/thaw cycles. At 24 and 48 h, 180 μL of media was sampled, 20 μL of IS was added, and tyrphostin A9 was extracted via liquid-liquid extraction. 20 μL of plasma was also sampled, 20 μL of IS was added, and then samples were diluted to 200 μL before liquid-liquid extraction. Samples were then vortexed, centrifuged, and dried under nitrogen before being evaluated to determine the percent recovery. In addition, the time course of benchtop stability in plasma was evaluated at 3 h, 6 h, and 24 h, as the recovery at 48 h was undetectable.

### 2.5. LC-MS/MS method conditions and validation criteria

Methods were developed and validated using a Waters Acquity LC with combined triple quadrupole mass spectrometry detector (TQD). The TQD was run in electrospray ionization negative mode. Multiple reaction monitoring was optimized with a cone voltage of 50 V and collision energy of 30 V. Masslynx software was used for machine operation and data analysis. A Waters Symmetry Shield RP8 (2.1 mm × 100 mm, 3.5 μm) was employed for separation with the conditions outlined in Table 1. The aqueous phase was composed of water: acetonitrile: acetic acid (95:5:0.1, v/v/v). The

**Table 1**
Liquid chromatography gradient conditions used for the separation of tyrphostin A9 and 3-(3,5-di-*tert*-butyl-4-hydroxyphenyl) propanoic acid.

| Time (min) | Aqueous (%) | Organic (%) |
|---|---|---|
| 0 | 50 | 50 |
| 2 | 50 | 50 |
| 5 | 5 | 95 |
| 7 | 5 | 95 |
| 7.1 | 50 | 50 |
| 10 | 50 | 50 |

organic phase was composed of water: acetonitrile: acetic acid (5:95:0.1, v/v/v). The column oven temperature was set to 25 °C to maintain a constant column temperature and the sample chamber was set to 4 °C. Method validation was carried out for each matrix by running standard curves and quality control samples with triplicate injections, on three separate days. Standards were freshly prepared, and QCs were prepared at an earlier time and stored at −20 °C. Inter-day and intra-day relative standard deviations (RSD) were calculated and determined to be acceptable if below 20%. Recovery of QCs between 75% and 120% and linearity greater than 0.99 were deemed acceptable. Limits of quantification (LOQ) and limits of detection (LOD) were calculated based on signal to noise ratios greater than 10 and 3 at the tyrphostin A9 transition (281.2 $m/z$ → 265.2 $m/z$) as previously described [14].

### 2.6. In vitro pharmacokinetics

An in vitro pharmacokinetic study was carried out with differentiated 3T3-L1 adipocytes. Following differentiation, cells were reseeded in 6-well plates at a density of ~$1 \times 10^6$ cells/well to maintain the confluency. Cells were incubated overnight to allow the cells to adhere to the plate. Following attachment, cells were exposed to 30 ng/mL of tyrphostin A9 in phenol red free DMEM with insulin. Media and cell samples were collected at 1, 3, 6, and 24 h after the addition of tyrphostin A9. Samples were prepared with the internal standard as described above and stored at −20 °C for later analysis.

### 2.7. Degradation samples

It is documented that tyrphostins are prone to hydrolysis [11]. In order to determine the potential degradation products of tyrphostin A9, a 24 h stability study was conducted in phenol red free media. 100 ng/mL of tyrphostin A9 in media was left at room temperature and protected from light for 24 h. Following 24 h, the predicted hydrolysis product, 3,5-di-*tert*-butyl-4-hydroxybenzaldehyde, was extracted from the samples as described below. The resulting peaks from the sample were then compared with the peak from a 100 ng/mL standard concentration of 3,5-di-*tert*-butyl-4-hydroxybenzaldehyde. For this analysis the LC conditions (buffers, gradient, and column) remained the same as the tyrphostin A9 analysis. However, the mass spectrometer was optimized for a single ion recording (SIR) method to detect the degradation product 3,5-di-*tert*-butyl-4-hydroxybenzaldehyde. This method requires only the optimization of the cone voltage which was found to be 48 V. The next step in method development was to determine extraction efficiency and sample preparation conditions. Since the chemical properties of 3,5-di-*tert*-butyl-4-hydroxybenzaldehyde are significantly different from tyrphostin A9, methanol was used in place of acetonitrile for extraction from the cell culture medium. Following extraction, samples were vortexed and centrifuged at 13,500 rcf for 10 min at 4 °C. 500 μL of each sample was transferred to glass test tubes and dried under nitrogen gas. Samples were reconstituted in water and acetonitrile (50:50, v/v) and subjected to further analysis.

## 3. Results

### 3.1. Method validation

#### 3.1.1. Specificity

Fig. 1A shows the representative chromatogram of cell culture media (blank matrix) and Fig. 1B shows the representative chromatogram and chemical structure of tyrphostin A9. Fig. 1C shows the combined total ion current chromatogram of both tyrphostin A9 and 3-(3,5-di-*tert*-butyl-4-hydroxyphenyl) propanoic acid, as well as the chemical structure of IS. Figs. 1D and E show the full-scan product ion mass spectra of IS and tyrphostin A9, respectively. Solvent blanks and matrix blanks contained no interfering peaks with the internal standard or tyrphostin A9, as shown in Fig. 1.

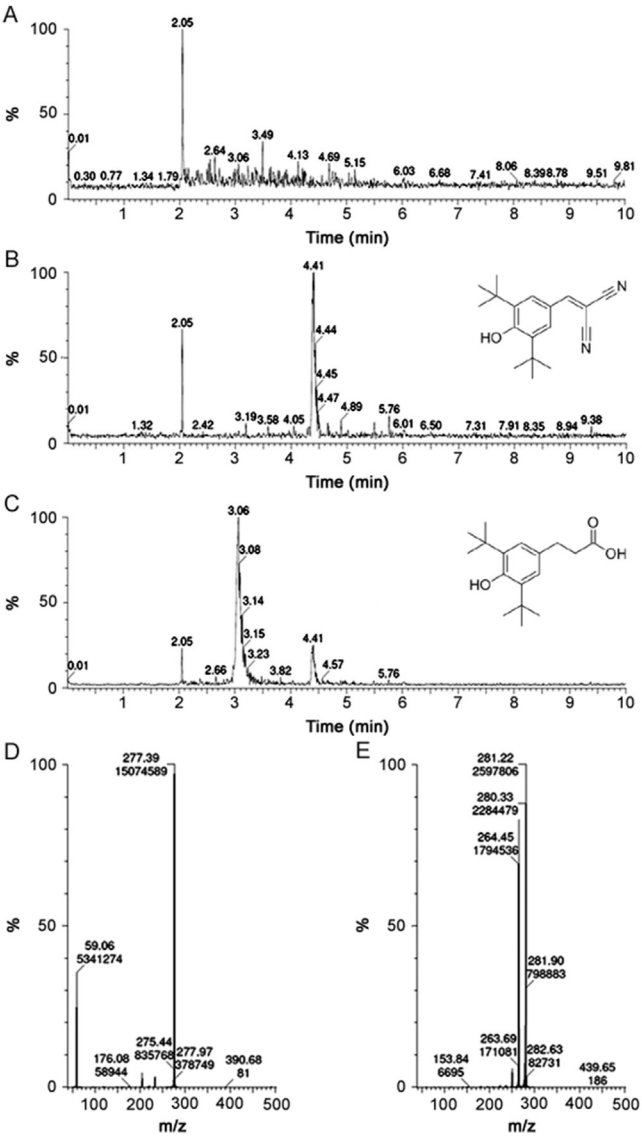


**Fig. 1.** LC-MS/MS chromatograms and mass spectra. (A) Chromatogram of blank media matrix from MRM negative mode. (B) Chromatogram of LLOQ tyrphostin A9 standard in cell culture media, analyzed in MRM negative mode, and structure of tyrphostin A9. (C) Total ion current (TIC) chromatogram of tyrphostin A9 and internal standard 3-(3,5-di-*tert*-butyl-4-hydroxyphenyl) propanoic acid, and the structure of internal standard. (D) Product ion scan mass spectra of 3-(3,5-di-*tert*-butyl-4-hydroxyphenyl) propanoic acid. (E) Product ion scan mass spectra of tyrphostin A9.

#### 3.1.2. Linearity, LOD, and LOQ

Representative standard curves for each of the three matrices are shown in Fig. 2. The linearity for each curve was found to be greater than 0.99 using a weighted least squares linear regression method. For each matrix the LOD was found to be 0.5 ng/mL and the LOQ was found to be 1.0 ng/mL.

#### 3.1.3. Precision and accuracy

Precision is the closeness of measured values to one another, and accuracy is the closeness of the measured value to the standard

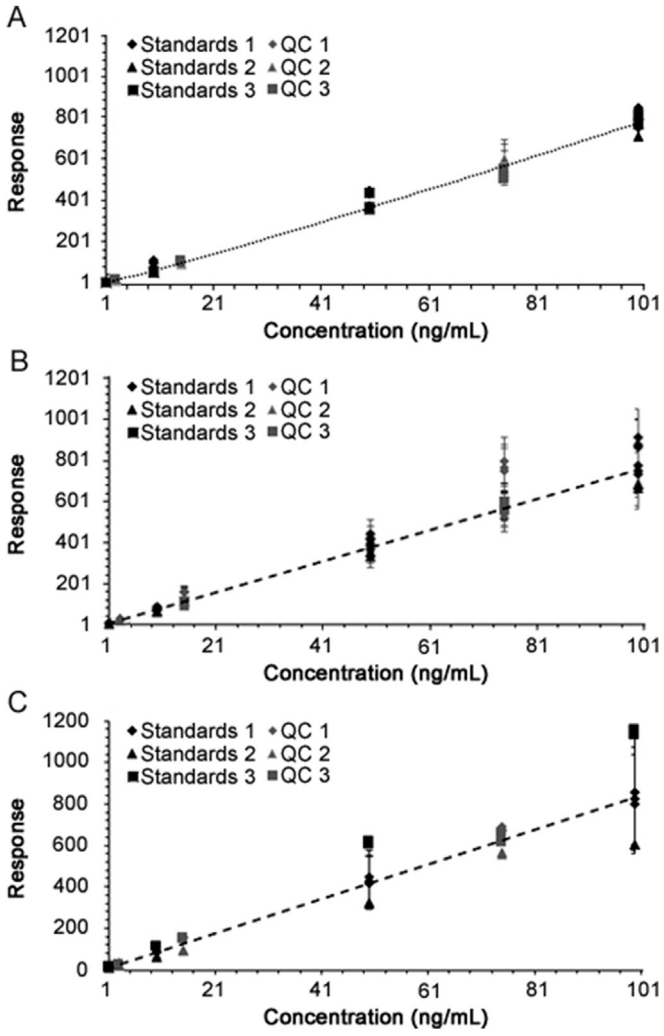


**Fig. 2.** Representative standard curves of tyrphostin A9 in various matrices. (A) Tyrphostin A9 standards and quality controls following extraction from cell culture media. (B) Tyrphostin A9 standards and quality controls following extraction from 3T3-L1 cell lysate. (C) Tyrphostin A9 standards and quality controls following extraction from murine plasma.

nominal concentration. Precision and accuracy were determined for both intra-day and inter-day standards. It was found that the standards maintained less than 20% relative standard deviation for the precision, and the accuracy fell between 79% and 102% (Table 2).

### 3.1.4. Matrix effects and recovery

Since matrix effects may enhance or diminish the ionization of the compound of interest, the matrix effect for tyrphostin A9 was evaluated by comparing the integrated peak signal of the compound at 100 ng/mL in the matrix vs. the solvent. All matrices were found to have greater than 70% signal recovery compared to the solvent. A summary of results for the matrix effect of cell culture media, 3T3-L1 cell lysate, and murine plasma is provided in Table 2. Recovery of tyrphostin A9 was assessed following sample preparation for each matrix. Briefly, the response from a matrix standard was compared with the response from a blank matrix spiked with tyrphostin A9 just before the analysis. All matrices demonstrated recovery around 100%.

## 3.2. Stability

As shown in Fig. 3A, following the incubation of tyrphostin A9 in cell culture media at room temperature for 48 h, the recovery was 49.6% when the samples were protected from the light and 36.7% when they were exposed to the light. Tyrphostin A9 was found to be completely degraded in the plasma at room temperature after 48 h. In order to determine the degradation kinetics of tyrphostin A9 in the plasma, additional samples were incubated at room temperature and collected at 3, 6, and 24 h. As shown in Fig. 3B, at 3 and 6 h only 15.8% and 10.4%, of tyrphostin A9 were left in the sample. By 24 h, the concentration of tyrphostin A9 in the plasma was below the LOQ.

## 3.3. In vitro pharmacokinetics

The single dose in vitro pharmacokinetic study was performed at 30 ng/mL concentration of tyrphostin A9, which has been shown to be above the uncoupling concentration of tyrphostin A9 in isolated rat mitochondria [12]. Results from the study are shown in Fig. 4. It was found that tyrphostin A9 concentrations in the media followed bi-exponential kinetics, whereas the concentrations inside the adipocytes remained constant around 2.5 ng/mL.

## 3.4. Degradation product

Previous work done by Won [11] has shown that tyrphostins readily undergo hydrolysis. The proposed hydrolysis products for tyrphostin A9 are outlined in Fig. 5, where the hydrolysis results in the formation of malononitrile and 3,5-di-*tert*-butyl-4-hydroxybenzaldehyde. To test this hypothesis, 100 ng/mL tyrphostin A9 sample was prepared in phenol red free cell culture media and incubated at room temperature for 24 h. The degradation products were extracted from the sample with methanol + 0.1%

**Table 2**
LC-MS/MS method validation results for tyrphostin A9 in cell culture media, 3T3-L1 cell lysate and murine plasma.

| Matrix | Nominal conc. (ng/mL) | Intra-day | | | Inter-day | | | LOD (ng/mL) | LOQ (ng/mL) | Linearity ($R^2$) | Recovery (%) | Matrix effect (%) |
|---|---|---|---|---|---|---|---|---|---|---|---|---|
| | | Mean conc. (ng/mL) | Accuracy (%) | Precision (% RSD) | Mean conc. (ng/mL) | Accuracy (%) | Precision (% RSD) | | | | | |
| Cell culture media | 3 | 2.56 | 85.3 | 2.82 | 2.37 | 79.2 | 8.64 | 0.5 | 1 | 0.995 | 100.3 | 82.4 |
| | 15 | 13.7 | 91.6 | 3.01 | 13.8 | 91.7 | 2.28 | | | | | |
| | 75 | 67.1 | 89.5 | 4.88 | 67.7 | 90.2 | 14.0 | | | | | |
| 3T3-L1 cell lysate | 3 | 2.98 | 99.2 | 4.38 | 3.41 | 86.2 | 12.1 | 0.5 | 1 | 0.999 | 101 | 71.6 |
| | 15 | 15.2 | 98.7 | 8.57 | 16.3 | 91.5 | 10.3 | | | | | |
| | 75 | 81.9 | 90.9 | 3.14 | 82.6 | 89.9 | 6.30 | | | | | |
| Murine plasma | 3 | 2.76 | 92.1 | 7.76 | 2.58 | 86.0 | 16.4 | 0.5 | 1 | 0.998 | 110 | 107 |
| | 15 | 16.4 | 109 | 2.59 | 14.5 | 96.3 | 1.6 | | | | | |
| | 75 | 73.8 | 98.4 | 1.64 | 76.5 | 102 | 11.9 | | | | | |

LOD: limit of detection, LOQ: limit of quantification.

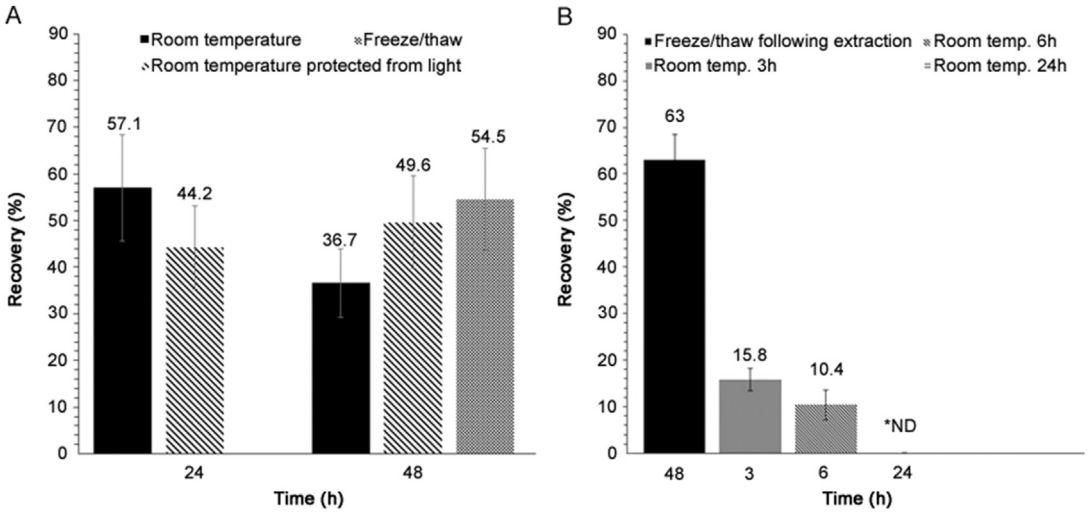


**Fig. 3.** Results from benchtop stability studies. (A) Stability of tyrphostin A9 in cell culture media left at room temperature, protected from light, and freeze-thaw cycle. (B) Stability of tyrphostin A9 in murine plasma following extraction and freeze/thaw cycle, and left at room temperature for 3 h, 6 h, and 24 h. ND: Not detected.

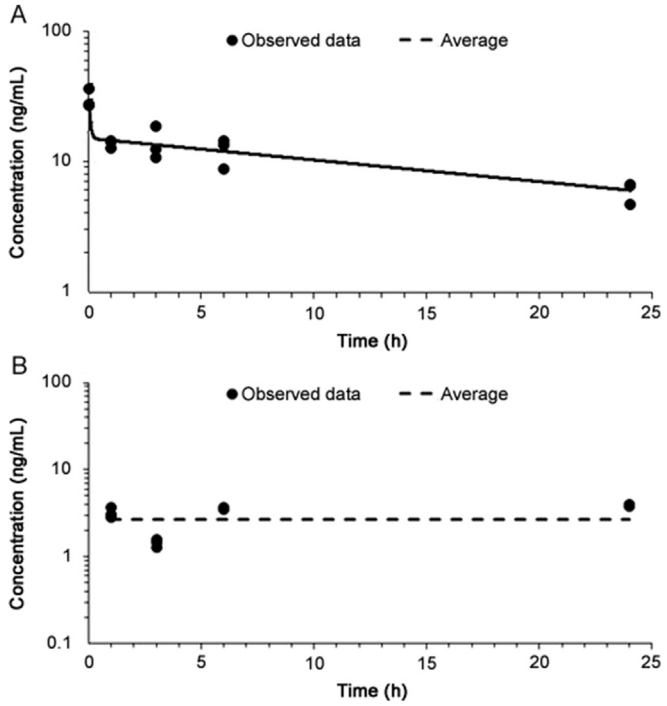


**Fig. 4.** In vitro pharmacokinetics of tyrphostin A9. (A) Media concentration vs. time profile of tyrphostin A9 for the duration of 24 h in the presence of 3T3-L1 adipocytes. (B) Measured 3T3-L1 intracellular concentration vs. time profile of tyrphostin A9 for up to 24 h.

formic acid and evaluated for the presence of 3,5-di-*tert*-butyl-4-hydroxybenzaldehyde. As shown in Fig. 6C, it was confirmed that tyrphostin A9 is degraded by hydrolysis, resulting in the formation of 3,5-di-*tert*-butyl-4-hydroxybenzaldehyde with the retention time of 3.89 min.

## 4. Discussion

Tyrphostin A9 has been explored in several early drug development scenarios; however, information about the stability and in vitro pharmacokinetics of tyrphostin A9 is lacking. The range of effective concentrations for tyrphostin A9 can be as low as 10 nM for the applications altering mitochondrial membrane potential, and as high as 150 nM for anti-influenza properties [7,12]. To facilitate further clinical development of this agent, we have developed an LC-MS/MS method that is sensitive enough to quantify the concentrations in nanomolar range.

One of the challenges faced during the development of this method was the selection of a suitable internal standard. Due to the lack of a commercially available deuterated tyrphostin A9, we tested a series of structurally similar compounds including tyrphostin 23, tyrphostin AG879, tyrphostin 1, butylated hydroxytoluene (BHT), butylated hydroxyanisole (BHA), 3-(3,5-di-*tert*-butyl-4-hydroxyphenyl) acetic acid, and 3-(3,5-di-*tert*-butyl-4-hydroxyphenyl) propanoic acid. Out of all these compounds 3-(3,5-di-*tert*-butyl-4-hydroxyphenyl) propanoic acid was found to be the most suitable internal standard because of its narrow peak shape and good recovery as shown in Fig. 1B. In addition, biological matrices may also contribute significant matrix effects due to decreased ionization efficiency of the compound of interest. The

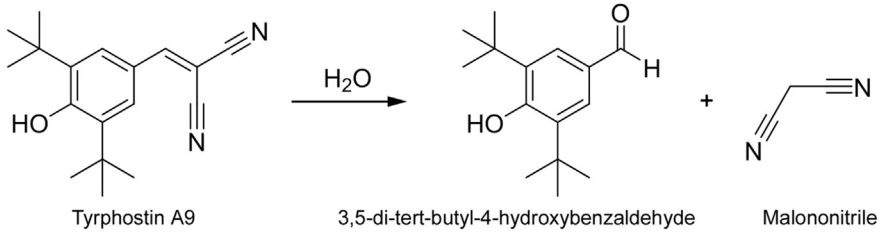


**Fig. 5.** Proposed degradation pathway of tyrphostin A9 through hydrolysis to form 3,5-di-*tert*-butyl-4-hydroxybenzaldehyde and malononitrile.

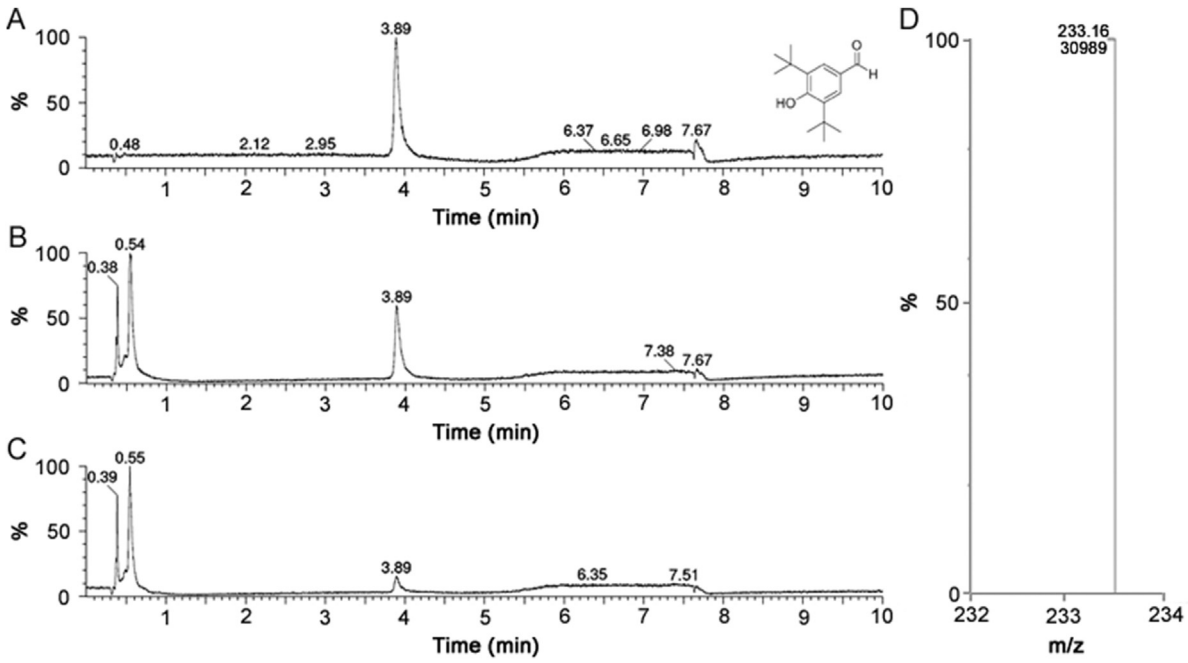


**Fig. 6.** Representative chromatograph of degradation product 3,5-di-*tert*-butyl-4-hydroxybenzaldehyde, at retention time of 3.89 min. (A) SIR scan of standard 3-(3,5-di-*tert*-butyl-4-hydroxyphenyl) propanoic acid in solvent (water:acetonitrile:acetic acid (50:50:0.1, v/v/v)). (B) Extracted 3,5-di-*tert*-butyl-4-hydroxybenzaldehyde standard from cell culture media. (C) Extracted 3,5-di-*tert*-butyl-4-hydroxybenzaldehyde following benchtop stability of tyrphostin A9 in cell culture media for 24 h. (D) Resulting mass spectra of 3,5-di-*tert*-butyl-4-hydroxybenzaldehyde from SIR scan.

phenol red component that is commonly used in cell culture media as a pH indicator caused significant ion suppression, and therefore, we proceeded to use phenol red free media.

Our goal was to develop an analytical method that can achieve sufficiently low LOQ to allow for the robust quantification of tyrphostin A9 at nanomolar concentration range, such as the concentration used for oxidative phosphorylation uncoupling. Following employment of a liquid-liquid extraction procedure, optimization of LC (Table 1), and MS/MS conditions (i.e. cone voltage of 50 V and collision energy of 30 V), the LOQ for our method was found to be 1 ng/mL. This value was ~50-fold lower than the LOQ reported for the analog Tyrphostin AG 1478 using an HPLC method [15]. In addition, the LOQ remained at 1 ng/mL for each of the three biological matrices tested (i.e. cell culture media, 3T3-L1 cell lysate and murine plasma), along with acceptable linearity, precision, and accuracy of the analytical method (Table 2).

In order to evaluate the practical application of our LC-MS/MS method, the stability of tyrphostin A9 was tested under different conditions in two matrices: cell culture media and murine plasma. Our results (Fig. 3) revealed that tyrphostin A9 is not stable in either matrix, and more susceptible to degradation in murine plasma compared to cell culture media. This difference may stem from the presence of enzymatic processes in the plasma. The addition of an esterase inhibitor may be necessary to stabilize plasma samples; however, this has not been investigated here. Degradation kinetics for tyrphostin A9 was found to be bi-phasic, which is consistent with the findings of Won [11]. We hypothesized that hydrolysis plays a major role in the degradation of tyrphostin A9, in both cell culture media and murine plasma. Fig. 6A depicts our proposed mechanism of tyrphostin A9 degradation. To confirm this hypothesis, we developed a single reaction monitoring (SIR) method that can identify the presence of the proposed hydrolysis product 3,5-di-*tert*-butyl-4-hydroxybenzaldehyde. Fig. 6A shows a representative chromatogram of 100 ng/mL 3,5-di-*tert*-butyl-4-hydroxybenzaldehyde. Due to the differences in the physicochemical properties of 3,5-di-*tert*-butyl-4-hydroxybenzaldehyde and tyrphostin A9, we utilized methanol with 0.1% formic acid to facilitate the extraction of 3,5-di-*tert*-butyl-4-hydroxybenzaldehyde from the media. Following the incubation of tyrphostin A9 in the cell culture media at room temperature for 24 h, the presence of 3,5-di-*tert*-butyl-4-hydroxybenzaldehyde was confirmed in the media (Fig. 6C), suggesting our hypothesis regarding rapid hydrolysis of tyrphostin A9 in biological matrices was correct. In addition to the metabolism of tyrphostin A9 itself, the products of tyrphostin A9 hydrolysis (shown in Fig. 5) may also be subject to further enzymatic degradation. Out of these products malononitrile may be of particular concern, as it has been shown to metabolize into cyanide in vivo by the liver, which can cause significant toxicities [16]. Of note, cyanide inhibits oxygen consumption in isolated rat hepatocytes with an EC50 value of 78 μM; therefore, large doses elevating concentrations of tyrphostin A9 may cause severe toxicity [17].

We also used our LC-MS/MS method to investigate in vitro pharmacokinetics of tyrphostin A9 in the adipocytes. Differentiated 3T3-L1 adipocytes were incubated with tyrphostin A9 for 24 h, and media as well as cell pellet were collected at different time points to measure tyrphostin A9 concentrations. It was found that tyrphostin A9 concentrations in the cell culture media remained above the LOQ for the duration of the 24 h (Fig. 4); however, these concentrations were lower than the observed concentration following the stability study in cell culture media alone after 48 h. This observation suggests that cellular distribution and/or metabolism of tyrphostin A9 may play an important role in determining the pharmacokinetics of the drug in the media in the presence of cells. In fact, throughout the 24 h of the study it was found that the concentration of tyrphostin A9 inside the adipocytes remained constant around 2.5 ng/mL. Since the pharmacokinetic profiles of tyrphostin A9 in the media and inside the cells were not parallel, this observation suggests that once inside the cell tyrphostin A9 may be protected from degradation or may be sequestered in a compartment (e.g. mitochondria) that allows the drug to remain

intact inside the cell for a longer period of time. Thus, our findings indicate the stability and role of pharmacokinetics should be considered for all in vitro experiments. Investigation into the cellular metabolism of tyrphostin A9 may be informative and the method presented here may serve as a useful tool to further quantitatively evaluate tyrphostin A9.

## 5. Conclusions

We have developed and validated a robust, selective, and sensitive LC-MS/MS method for the quantification of tyrphostin A9 in cell culture media, 3T3-L1 cell lysate, and murine plasma. The LOQ for tyrphostin A9 was found to be 1 ng/mL for each biological matrix tested. The LC-MS/MS method was further applied to investigate the stability and in vitro pharmacokinetics of tyrphostin A9. It was found that similar to other tyrphostins, tyrphostin A9 is susceptible to hydrolysis, and the hydrolysis product was confirmed to be 3,5-di-*tert*-butyl-4-hydroxybenzaldehyde. It was also found that tyrphostin A9 is more susceptible to degradation in murine plasma compared to cell culture media, which may be due to the presence of enzymes in the plasma. In vitro pharmacokinetics studies revealed that tyrphostin A9 concentrations in the cell culture media declined faster in the presence of adipocytes, whereas the concentrations inside the adipocytes remained constant throughout the study. This observation suggests that once inside the cell tyrphostin A9 may be protected from degradation. Thus, further work is needed to elucidate the potential of tyrphostin A9 as a potential therapeutic.

## Acknowledgments

This work was supported by NIH grant GM114179 and AI138195 to D.K.S. and the Centre for Protein Therapeutics at University at Buffalo. L.F.M would like to acknowledge Donald F. and Edna G. Bishop Scholarship Foundation for their continued support. The authors would also like to thank Donna Ruszaj for her help in finding the suitable internal standard for the analysis.

## Conflicts of interest

Authors declare that there are no conflicts of interest.

## References

[1] A. Gazit, P. Yaish, C. Gilon, et al., Tyrphostins I: synthesis and biological activity of protein tyrosine kinase inhibitors, J. Med. Chem. 32 (1989) 2344–2352.
[2] M.L. Bond, A. Azzolina, E.F. Craparo, et al., Entrapment of an EGFR inhibitor into nanostructured lipid carriers (NLC) improves its antitumor activity against human hepatocarcinoma cells, J. Nanobiotechnol. 12 (2014) 21.
[3] K. Iida, K. Nakayama, M.T. Rahman, et al., EGFR gene amplification is related to adverse clinical outcomes in cervical squamous cell carcinoma, making the EGFR pathway a novel therapeutic target, Br. J. Canc. 105 (2011) 420–427.
[4] A. Novogrodsky, M. Weisspapir, M. Patya, et al., Tyrphostin 4-nitrobenzylidene malononitrile reduces chemotherapy toxicity without impairing efficacy, Cancer Res. 58 (1998) 2397–2403.
[5] Q. Chen, A.A. Luo, H. Qiu, et al., Monocyte interaction accelerates HCl-induced lung epithelial remodeling, BMC Pulm. Med. 14 (2014) 135.
[6] N. Kumar, Y. Liang, T.G. Parslow, et al., Receptor tyrosine kinase inhibitors block multiple steps of influenza A virus replication, J. Virol. 85 (2011) 2818–2827.
[7] N. Kumar, N.R. Sharma, H. Ly, et al., Receptor tyrosine kinase inhibitors that block replication of influenza A and other viruses, Antimicrob. Agents Chemother. 55 (2011) 5553–5559.
[8] S.J. Park, Y.J. Park, J.H. Shin, et al., A receptor tyrosine kinase inhibitor, tyrphostin A9 induces cancer cell death through Drp1 dependent mitochondria fragmentation, Biochem. Biophys. Res. Commun. 408 (2011) 465–470.
[9] Y. Sagara, K. Ishige, C. Tsai, et al., Tyrphostins protect neuronal cells from oxidative stress, J. Biol. Chem. 277 (2002) 36204–36215.
[10] A.R. Anand, A. Prasad, R.R. Bradley, et al., HIV-1 gp120-induced migration of dendritic cells is regulated by a novel kinase cascade involving Pyk2, p38 MAP kinase, and LSP1, Blood 114 (2009) 3588–3600.
[11] C.M. Won, Kinetics and mechanism of hydrolysis of tyrphostins, Int. J. Pharm. 104 (1994) 29–40.
[12] H. Terada, Uncouplers of oxidative phosphorylation, Environ. Health Perspect. 87 (1990) 213–218.
[13] K. Zebisch, V. Voigt, M. Wabitsch, et al., Protocol for effective differentiation of 3T3-L1 cells to adipocytes, Anal. Biochem. 425 (2012) 88–90.
[14] G. Tiwari, R. Tiwari, Bioanalytical method validation: an updated review, Pharm. Meth. 1 (2010) 25.
[15] A.G. Ellis, E.C. Nice, J. Weinstock, et al., High-performance liquid chromatographic analysis of the tyrphostin AG1478, a specific inhibitor of the epidermal growth factor receptor tyrosine kinase, in mouse plasma, J. Chromatogr. B Biomed. Sci. Appl. 754 (2001) 193–199.
[16] C.C. Willhite, R.P. Smith, The role of cyanide liberation in the acute toxicity of aliphatic nitriles, Toxicol. Appl. Pharmacol. 59 (1981) 589.
[17] S.J. Gee, C.E. Green, C.A. Tyson, Cyanide-induced cytotoxicity to isolated hepatocytes, Toxicol. In Vitro 4 (1990) 37–45.